nature biotechnology

CRISPR–Cas9 epigenome editing enables high-throughput screening for functional regulatory elements in the human genome

Tyler S Klann[1,2], Joshua B Black[1,2], Malathi Chellappan[1,2], Alexias Safi[2], Lingyun Song[2], Isaac B Hilton[1,2], Gregory E Crawford[2,3], Timothy E Reddy[1,2,4] & Charles A Gersbach[1,2,5]

Large genome-mapping consortia and thousands of genome-wide association studies have identified non-protein-coding elements in the genome as having a central role in various biological processes. However, decoding the functions of the millions of putative regulatory elements discovered in these studies remains challenging. CRISPR–Cas9-based epigenome editing technologies have enabled precise perturbation of the activity of specific regulatory elements. Here we describe CRISPR–Cas9-based epigenomic regulatory element screening (CERES) for improved high-throughput screening of regulatory element activity in the native genomic context. Using dCas9^{KRAB} repressor and dCas9^{p300} activator constructs and lentiviral single guide RNA libraries to target DNase I hypersensitive sites surrounding a gene of interest, we carried out both loss- and gain-of-function screens to identify regulatory elements for the β-globin and HER2 loci in human cells. CERES readily identified known and previously unidentified regulatory elements, some of which were dependent on cell type or direction of perturbation. This technology allows the high-throughput functional annotation of putative regulatory elements in their native chromosomal context.

Understanding how the human genome transforms dynamic biological signals into complex patterns of gene expression remains a fundamental challenge for biological research. Overcoming that challenge is especially important for improving the ability to treat human disease, as >90% of the genetic variation associated with complex disease falls within the noncoding genome[1,2]. Large annotation efforts such as ENCODE[3] and the US National Institutes of Health Roadmap Epigenomics Program[4] have revealed millions of putative regulatory elements across >100 human cell types that contribute to the transformation of biological signals into cellular responses and phenotypes[1]. The potential functions of those elements are typically unknown, however, because there are not sufficiently high-throughput assays to measure endogenous regulatory element activity or to link that activity to specific functions and target genes. High-throughput massively parallel reporter assays have been effective in quantifying the activity of regulatory elements in particular cell types[5–7], but they do not recapitulate regulatory element interactions at the native chromosomal locus and cannot identify the target genes of each element. Until recently, direct interrogation of these critical regulatory regions in their native chromosomal position has not been possible.

The type II clustered, regularly interspaced, short palindromic repeat/CRISPR-associated protein 9 (CRISPR–Cas9) system is a versatile tool for genome engineering[8–12]. Genome editing tools, including Cas9 and pooled guide RNA (gRNA) libraries, have also been used for high-throughput loss-of-function screens of genes[13–15] and regulatory elements[16–21]. Such CRISPR–Cas9 screens rely on ablation of the activity of critical regions, such as transcription-factor-binding sites, by the introduction of short insertions or deletions of DNA following Cas9-induced cleavage of the genome and repair by nonhomologous end joining. Consequently, a high density of gRNAs is needed to saturate all possible transcription-factor-binding sites in each regulatory element. In many cases, this degree of saturation is not possible because a protospacer-adjacent motif sequence is not located within the transcription-factor-binding sequence. Finally, screening of regulatory elements with genome editing examines loss-of-function by genomic disruption only, and does not permit gain-of-function analyses[22].

Nuclease-deactivated Cas9 (dCas9) can be fused to epigenome-modifying protein domains to precisely modulate gene expression from gene promoters and both proximal and distal genomic enhancer regions[23–37]. Additionally, repressor- or activator-domain fusions to dCas9 combined with pools of gRNAs that target gene promoters have been used for genome-wide CRISPR-interference and CRISPR-activation screens[28,29]. Here we focus on the dCas9-based transcriptional repressor dCas9^{KRAB} and the transcriptional activator dCas9^{p300}. Fusion of the KRAB (Krüppel-associated box) domain to dCas9 and subsequent targeting to a promoter or enhancer causes highly specific gene repression through the recruitment of a host of factors

[1]Department of Biomedical Engineering, Duke University, Durham, North Carolina, USA. [2]Center for Genomic and Computational Biology, Duke University, Durham, North Carolina, USA. [3]Department of Pediatrics, Division of Medical Genetics, Duke University Medical Center, Durham, North Carolina, USA. [4]Department of Biostatistics and Bioinformatics, Duke University Medical Center, Durham, North Carolina, USA. [5]Department of Orthopaedic Surgery, Duke University Medical Center, Durham, North Carolina, USA. Correspondence should be addressed to T.E.R. (tim.reddy@duke.edu), G.E.C. (greg.crawford@duke.edu) or C.A.G. (charles.gersbach@duke.edu).

Received 19 September 2016; accepted 17 March 2017; published online 3 April 2017; doi:10.1038/nbt.3853

that deposit trimethylation of histone H3 on Lys9 (H3K9me3), which ultimately results in heterochromatin formation[24,32]. Conversely, fusion of the E1A-associated protein p300 histone acetyltransferase core domain to dCas9 and targeting to either promoters or enhancers induces target gene activation concomitant with the deposition of acetylation of histone H3 on Lys27 (H3K27ac)[30]. Because screening with epigenome editing perturbs regulatory element activity directly rather than via DNA mutation, the approach offers several advantages over genome editing screens. Epigenome editing can modulate regulatory element activity even if there is not a protospacer-adjacent motif precisely within a critical transcription-factor-binding motif. Fewer gRNAs may be needed to achieve robust modulation of each candidate regulatory element, thus enabling the screening of a larger number of genomic regions with a fixed gRNA library size (**Supplementary Table 1**). Finally, the dCas9^{p300} tool provides an opportunity to screen for gain of regulatory element function that is not possible with genome editing mediated by nonhomologous end joining, even if the specific transcription factors that bind the element when active are not present in the cell type being studied[30]. The use of dCas9^{KRAB} and dCas9^{p300} in parallel screens around the same loci uniquely facilitates the identification of elements that are necessary and sufficient, respectively, for target gene expression.

DNase I hypersensitivity sequencing (DNase-seq) is a genome-wide, transcription-factor-agnostic measure of chromatin accessibility, corresponding to genomic loci where proteins are bound to DNA[38,39]. Many of the ~2 million DNase I hypersensitive sites (DHSs) that have been identified across many human cell and tissue types are likely to be regulatory elements that influence gene expression, and many of these are cell-type specific[1]. However, systematic identification and quantification of the effects of these regulatory elements on gene expression levels has not been possible. Here we demonstrate the utility of CERES by targeting DHSs surrounding genes of interest to identify endogenous regulatory elements through loss- and gain-of-function epigenome editing.

RESULTS

Epigenetic repression recovers known regulatory elements

We first designed pools of gRNAs to specifically target all DHSs in a particular segment of the genome. We identified protospacer sequences within each DHS surrounding the gene of interest, and ranked them by possible off-target alignments (Online Methods). The gRNA library pool was synthesized and cloned into a lentiviral expression vector used to generate a pool of lentiviral particles that delivered individual gRNAs to the target cells[16,17] (**Fig. 1a**).

We screened for regulatory elements within the well-characterized β-globin locus. The β-globin locus control region (LCR) contains five DHSs (HS1–5) upstream of five globin genes (*HBE1*, *HBG1*, *HBG2*, *HBD*, and *HBB*)[40]. This LCR controls the expression of each gene at different times throughout development in erythroid cells[41]. The K562 myelogenous leukemia cell line has high expression of *HBE1*

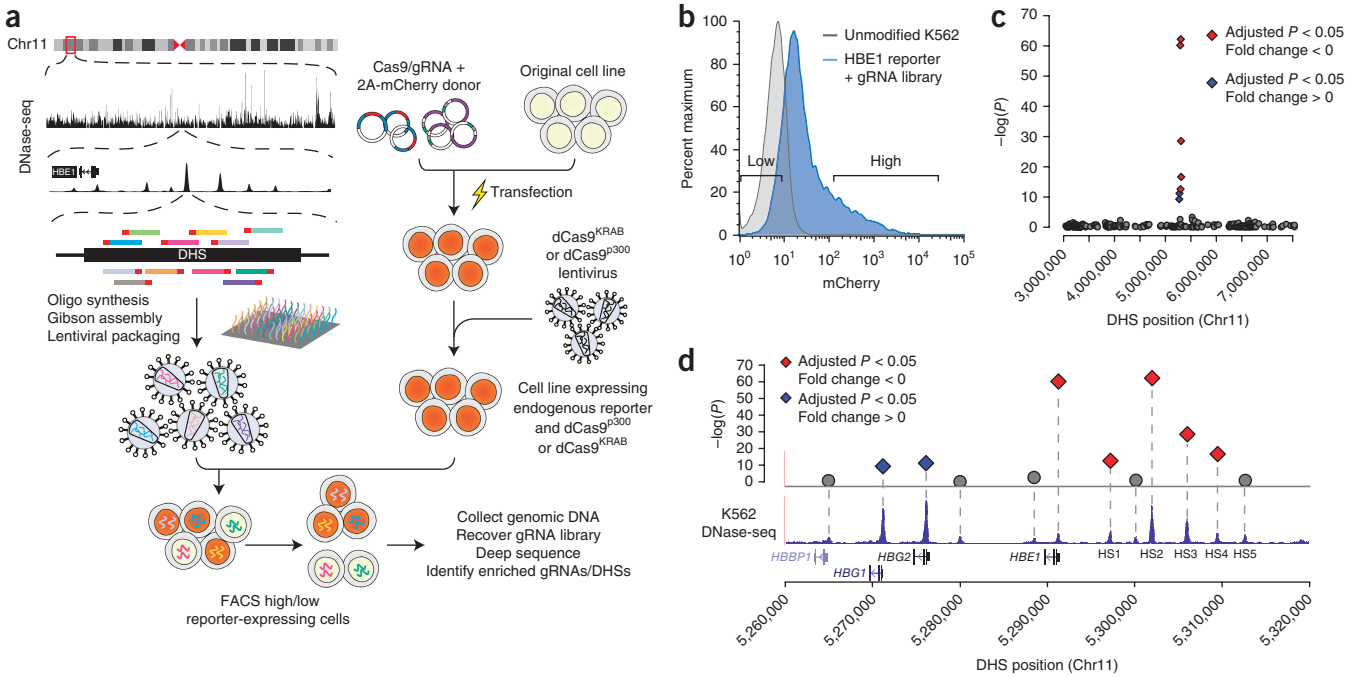

Figure 1 CRISPR–Cas9-based epigenetic regulatory element screening (CERES) identifies regulatory elements of the β-globin locus in a loss-of-function screen. (**a**) CERES involves the design and synthesis of libraries of gRNAs targeted to all candidate gene regulatory elements in a genomic region, in this case as defined by DHSs identified by DNase-seq. Lentiviral vectors encoding the gRNA library are delivered to cell lines that express the dCas9^{KRAB} repressor for loss-of-function screens, or the dCas9^{p300} activator for gain-of-function screens. The cells can then be selected for changes in phenotype, such as gain or loss of expression of a target gene. Sequencing the gRNAs in the selected cell subpopulations and mapping them back to the genome reveals the regulatory elements involved in controlling the selected phenotype. In the example shown here, a gRNA library was designed to all DHSs in a 4.5-Mb region surrounding the β-globin locus, and introduced into human K562 cells expressing dCas9^{KRAB} and containing an mCherry reporter at *HBE1*. FACS, fluorescence-activated cell sorting. (**b**) Representative flow cytometry data for the *HBE1* reporter cells containing the gRNA library, and expression levels (low versus high) of cells sorted for gRNA enrichment. (**c**) Manhattan plot of a high-throughput screen for regulatory elements in the 4.5 Mb surrounding the globin locus, using the dCas9^{KRAB} repressor. (**d**) Enriched DHSs after selection for decreased *HBE1* expression were found only in the *HBE1* promoter and enhancers (HS1–4), whereas the promoters of *HBG1*/*2* were enriched in cells with increased *HBE1* expression. Diamonds and circles in **c** and **d** represent individual DHSs; gray circles represent adjusted $P > 0.05$. Red indicates DHS fold change < 0, and blue indicates DHS fold change > 0.

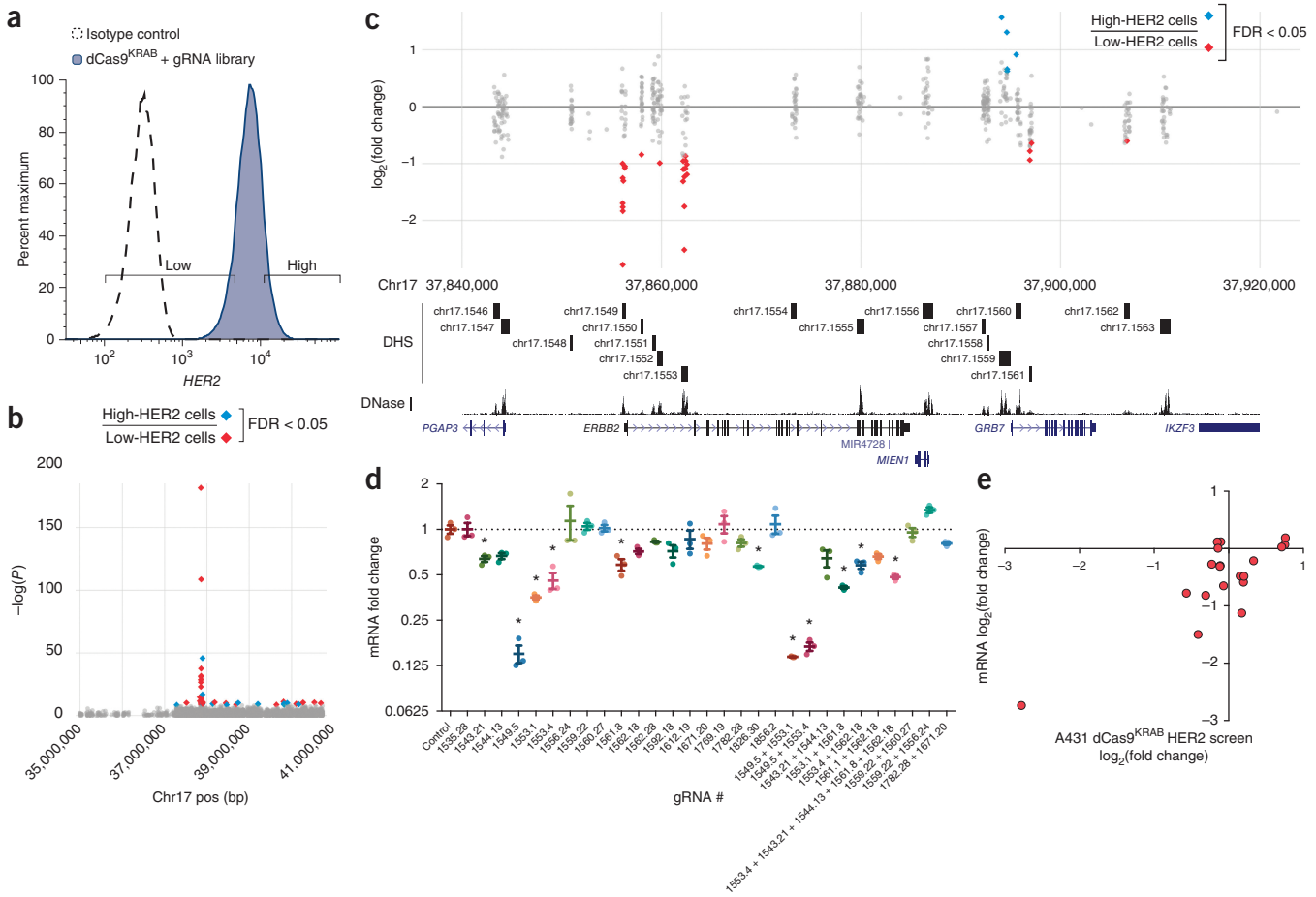

Figure 2 A dCas9^{KRAB} loss-of-function screen in A431 cells identified regulatory elements of *HER2*. (**a**) Flow cytometry for *HER2* expression in A431 cells expressing dCas9^{KRAB} and a gRNA library targeted to all DHSs in the 4 Mb surrounding *HER2* detected in the HER2-overexpressing SKRB3 breast cancer cell line. (**b**) Manhattan plot showing gRNAs in regulatory elements affecting HER2 expression. (**c**) A detailed view of the region around *HER2*. Comparison of cell populations with high and low HER2 expression showed that gRNAs are enriched in the promoter and an intronic DHS of HER2, as well as in surrounding DHSs, including the promoter of *GRB7*, an adaptor protein that associates with tyrosine kinases. (**d**) *HER2* mRNA fold change in response to the most enriched gRNAs from **b**, relative to treatment with a control gRNA. Asterisks indicate adjusted $P < 0.05$ versus control, one-way analysis of variance followed by Dunnett's test ($n = 3$ biological replicates; mean ± s.e.m.). (**e**) *HER2* mRNA $\log_2$ fold change in response to gRNA treatment versus $\log_2$ fold change of the abundance of the corresponding gRNA in the HER2 dCas9^{KRAB} screen (Spearman correlation $\rho = 0.5175$) Diamonds and circles in **b**,**c**,**e** represent individual gRNAs. Gray circles (**b**,**c**) represent gRNAs that were not significantly enriched.

and *HBG1/2* and has accessible chromatin at all five DHSs in the β-globin LCR[42]. We previously demonstrated robust modulation of *HBE1* expression by epigenome editing of the HS2 enhancer[30,32]. To more easily monitor the transcriptional modulation of *HBE1*, we generated an endogenous reporter in K562 cells by replacing the stop codon of *HBE1* with a P2A–mCherry sequence via CRISPR–Cas9-mediated genome editing. We then transduced these reporter cells with a lentivirus encoding dCas9^{KRAB} and derived clonal isogenic populations from single cells (**Fig. 1a**). To test for proper reporter activity, we transduced cells individually with four different gRNAs targeting the HS2 enhancer, and we used flow cytometry to verify reduced mCherry expression (**Supplementary Fig. 1** and **Supplementary Table 2**).

We used DNase-seq data from K562 cells[43] to design a library of 10,739 gRNAs targeting 281 DHSs in a 4.5-Mb region surrounding the β-globin locus, and 1,733 control gRNAs targeting regions between DHSs in this region. We transduced the *HBE1* reporter cell line at a low multiplicity of infection (MOI) to introduce one gRNA per cell, and after 2 d we added blasticidin S and then cultured for an additional 12 d to select for gRNA-containing cells. We carried out fluorescence-activated cell sorting to isolate the cells with mCherry expression levels in the top and bottom 10% (**Fig. 1b**). As a control, we also collected unsorted cells. We then used high-throughput sequencing to estimate the relative abundance of each gRNA in the genomic DNA of each sample. We identified DHSs involved in *HBE1* regulation by grouping gRNAs within a DHS as replicates and using linear regression to identify DHSs with significant differences in gRNA abundance between the high- and low-mCherry cell populations. Notably, the only DHSs that were significantly enriched within the low-*HBE1* library were four of the β-globin LCR enhancers, HS1–4, and the promoter of *HBE1* (**Fig. 1c**,**d**). The *HBG1/2* promoters were significantly (adjusted $P < 0.05$) enriched in the high-*HBE1* population, which indicates that repression of *HBG1/2* promoters leads to upregulation of *HBE1*, potentially by relieving competition between the promoters for the HS1–5 enhancers.

As an alternative analysis strategy, we determined the enrichment of individual gRNAs and detected similar trends, with the strongest enrichment in the *HBE1*, *HBG1/2* promoter, and HS1–4 enhancer regions (**Supplementary Fig. 2**). Control gRNAs outside the regions of DNase I signal in K562 cells, including gRNAs interspersed between HS1 and HS4, were not significantly enriched. We validated our results by individually delivering

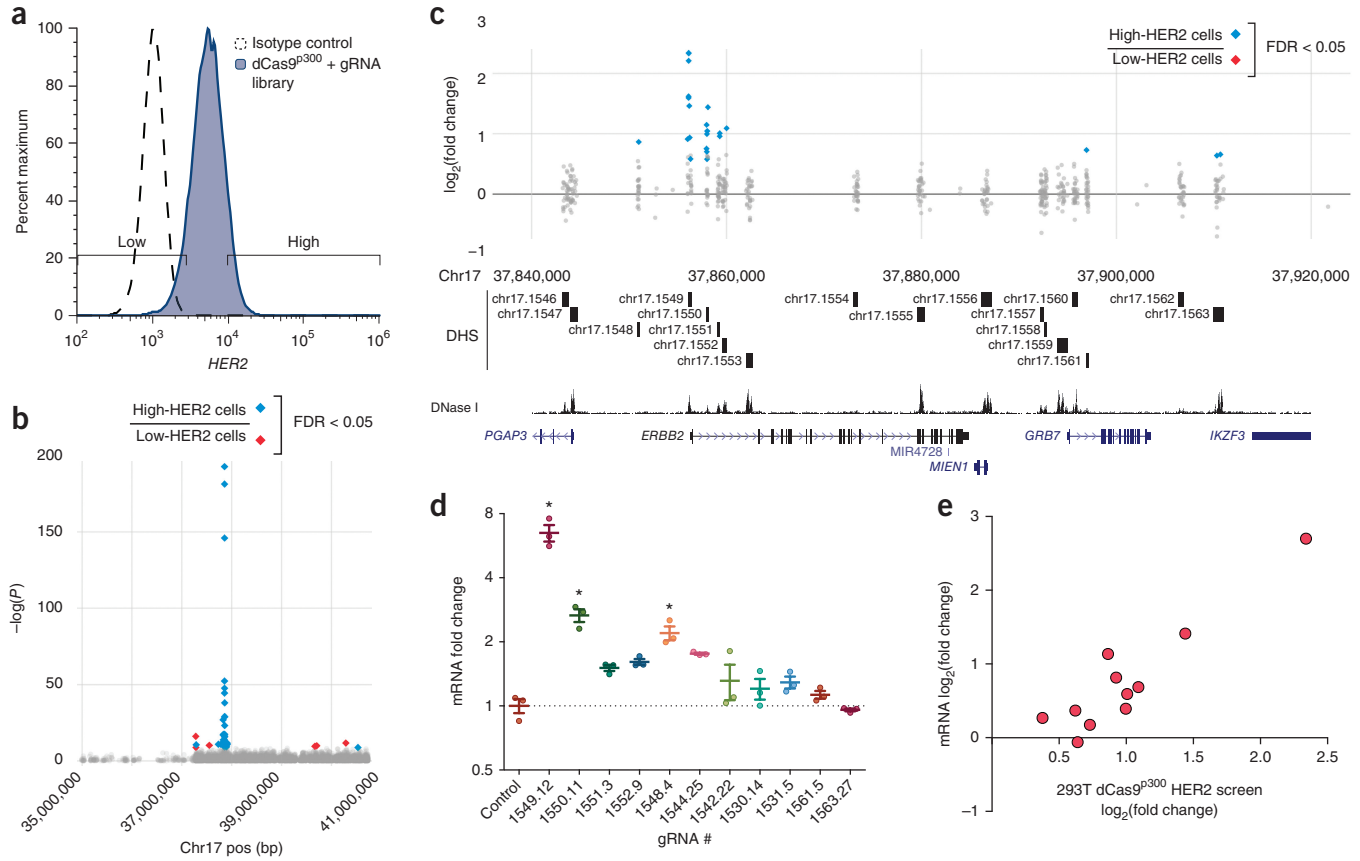

Figure 3 A dCas9^{p300} gain-of-function screen in HEK293T cells identified regulatory elements of *HER2*. (**a**) Flow cytometry for *HER2* expression in HEK293T cells expressing dCas9^{p300} and a gRNA library targeted to all the DHSs in a 4-Mb region surrounding *HER2* found in the SKBR3 HER2-overexpressing breast cancer cell line. (**b**) Manhattan plot showing the results of a screen for regulatory elements affecting HER2 expression. (**c**) A detailed view of the region around *HER2*. Comparison of cell populations with high and low HER2 expression showed that gRNAs are enriched in the promoter and three intronic DHSs of *HER2*, as well as in several nearby DHSs. (**d**) *HER2* mRNA fold change in response to the most enriched gRNAs from **b** relative to treatment with a control gRNA. Asterisks indicate adjusted $P < 0.05$ versus control, one-way analysis of variance followed by Dunnett's test ($n = 3$ biological replicates, mean ± s.e.m.). (**e**) *HER2* mRNA $\log_2$ fold change in response to gRNA treatment versus $\log_2$ fold change of the abundance of the corresponding gRNA in the HER2 HEK293T dCas9^{p300} screen (Spearman correlation $\rho = 0.9429$). Diamonds and circles in **b**,**c**,**e** indicate individual gRNAs. Diamonds represent significantly enriched gRNAs (adjusted $P < 0.05$). Red diamonds represent $\log_2$(fold change) < 0, and blue diamonds represent $\log_2$(fold change) > 0. Gray circles in **b**,**c** represent gRNAs that were not significantly enriched.

the most differentially enriched gRNAs of each significant DHS under the same conditions as used in the screen. We then measured the fold change of mCherry expression and *HBE1* mRNA levels by flow cytometry and RT-qPCR, respectively. We observed high correlation of both measurements (Spearman $\rho = 0.9429$ and 0.8857, respectively) with the $\log_2$(fold change) of the individual gRNAs from the screen (**Supplementary Fig. 3**).

Epigenetic repression reveals gene regulatory elements

We next extended this approach to identify regulatory elements of *HER2* (*ERBB2*; also known as *Neu*), an oncogene that is overexpressed or amplified in approximately 20–30% of breast cancers[44]. *HER2*-positive breast cancer has the second-poorest prognosis rate of all subtypes. The HER2 humanized monoclonal antibody trastuzumab is part of the standard-of-care treatment and can improve survival by 20–25 months[45]. However, less than 35% of patients initially respond to treatment, and 70% of those who do respond can develop resistance to the drug, often as a result of protein regulation[44,46]. This provides an attractive target for screens for the regulatory regions that may be controlling *HER2* expression.

To design the gRNA library, we generated DNase-seq data for the SKBR3 *HER2*-amplified breast cancer cell line and used the DHS coordinates as input to identify gRNAs. We generated a pooled gRNA library as described above; the final library contained 12,189 gRNAs targeting 433 DHSs in a 4-Mb region surrounding *HER2*, and 283 control gRNAs within that same region that did not target DHSs. Because HER2 is a transmembrane protein, we used immunofluorescence staining to monitor expression, as an alternative to generating an endogenous reporter cell line. We transduced A431 epidermoid carcinoma cells, which express moderate levels of HER2, with dCas9^{KRAB} lentivirus and selected for stable expression. We then transduced the selected, polyclonal A431-dCas9^{KRAB} cells with the gRNA library at low MOI and selected for the gRNA vector with antibiotic. Next, we used flow cytometry to sort cells with HER2 levels in the top and bottom 10% (**Fig. 2a**). We sequenced gRNAs and performed enrichment analysis. When we compared the samples with the highest HER2 expression to those with the lowest, we identified several DHSs containing individual gRNAs that were differentially represented between the two groups (**Fig. 2b**,**c**), as well as DHSs that were called when we used individual gRNAs as replicates within a DHS (**Supplementary Fig. 4**). Enrichment in the low-HER2 population included the *HER2* promoter; several DHSs in the first intron of *HER2*, including one previously identified regulatory element[47]; and several DHSs downstream of *HER2*, including one DHS in the first intron of *GRB7*. In high-HER2 cells, we detected enrichment of gRNAs in two DHSs near

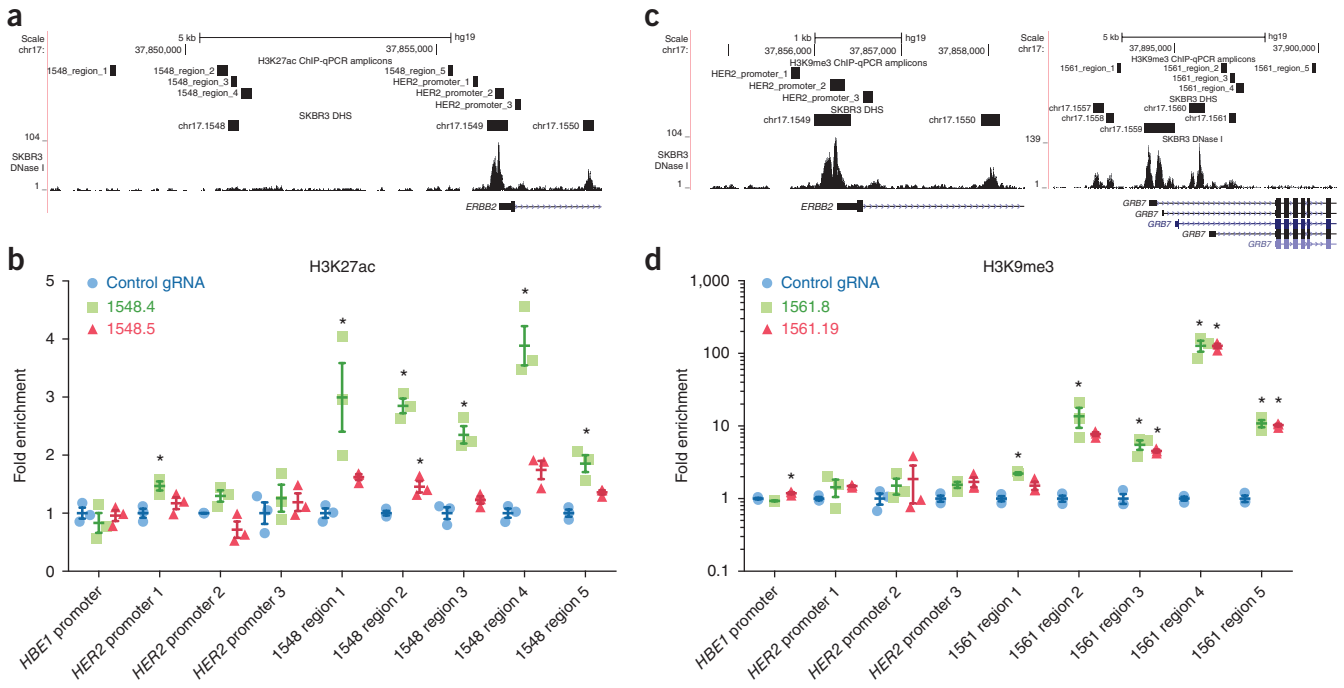

Figure 4 dCas9^{p300} and dCas9^{KRAB} remodel epigenetic marks near novel regulatory elements identified from screens. (**a**) Genomic tracks displaying the qPCR amplicon regions for the H3K27ac ChIP-qPCR assay, DNase-seq signal, and DHSs for SKBR3 cells near *HER2*. (**b**) dCas9^{p300} targeted to a DHS with a gRNA enriched in the screen (1548.4) in HEK293T cells led to H3K27ac enrichment near the DHS, in contrast to gRNA 1548.5, which targets the same DHS but was not enriched in the screen. (**c**) Genomic tracks displaying the qPCR amplicon regions for the H3K9me3 ChIP-qPCR assay, DNase-seq signal, and DHSs for SKBR3 cells near *HER2* and *GRB7*. (**d**) dCas9^{KRAB} targeted to a DHS with a gRNA enriched in the screen (1561.8) in A431 cells deposited H3K9me3 near the DHS. A gRNA that was not significantly enriched in the screen (1561.19) also deposited similar amounts of H3K9me3 near the DHS. Asterisks in **b** and **d** indicate adjusted $P < 0.05$ versus control, one-way analysis of variance followed by Dunnett's test ($n = 3$ biological replicates, mean ± s.e.m.). All fold enrichments are relative to the transduction of a control gRNA and normalized to a region of the *ACTB* locus.

the promoter of *GRB7*. We also found that the relative expression of *GRB7* mRNA was significantly ($P < 0.05$) reduced when targeting the promoter or first intron of *GRB7* (**Supplementary Fig. 5**). Therefore, the regulation of HER2 levels via the DHSs in the *GRB7* promoter may be due to relief of the competition of distal enhancers, or possibly to post-transcriptional secondary effects, as GRB7 is involved in the phosphorylation of HER2 (ref. 48). To validate the screen, we delivered several of the most enriched gRNAs individually to the same A431-dCas9^{KRAB} cells. We again found a high degree of correlation between the fold change of *HER2* mRNA or protein levels, determined by RT-qPCR (Spearman ρ = 0.5175) or immunofluorescence staining (ρ = 0.5701), respectively, and the $\log_2$(fold change) of gRNA representation in the screen (**Fig. 2d**,**e** and **Supplementary Fig. 5b**; $P < 0.05$).

Epigenetic activation reveals gene regulatory elements

One application of epigenome editing is the targeted activation of regulatory elements in their natural chromosomal position. This provides the unique opportunity to identify regulatory elements that induce the expression of a gene that is not normally expressed in a particular cell type. To extend CERES to gain-of-function screens for regulatory elements sufficient to activate target gene expression, we used the dCas9^{p300} activator[30]. We transduced human HEK293T cells, which express low levels of HER2, with dCas9^{p300} lentivirus and selected with antibiotic to obtain a polyclonal cell line that stably expressed the transgene. We then transduced the HEK293T-dCas9^{p300} cells with the same gRNA library used in the A431-dCas9^{KRAB} screen, targeting the 4-Mb region around *HER2*. At 2 d after transduction, we initiated a 7-d antibiotic selection to select cells that contained the gRNA vector. We then sorted the cells for high and low HER2 expression (**Fig. 3a**). We observed a profile that largely mirrored the dCas9^{KRAB} screen, with effects in the opposite direction, including enrichment of individual gRNAs (**Fig. 3b**,**c**) and DHSs (**Supplementary Fig. 6**), using each gRNA as a replicate, in the promoter region and first intron of *HER2*. We individually validated the most enriched gRNAs in HEK293T-dCas9^{p300} cells and detected a high degree of correlation of both mRNA fold change (Spearman ρ = 0.7818) and protein abundance (ρ = 0.8545) with the $\log_2$(fold change) of gRNA abundance in the screen (**Fig. 3d**,**e** and **Supplementary Fig. 7a**,**b**). To confirm that gene regulation at these DHSs was associated with the intended epigenetic editing by dCas9^{KRAB} and dCas9^{p300}, we carried out chromatin immunoprecipitation coupled with quantitative PCR (ChIP-qPCR) to validate the enrichment of H3K9me3 and H3K27ac, respectively (**Fig. 4**).

Screen results depend on cell type and direction of perturbation

The strongest intronic DHS (DHS_1553) identified in the dCas9^{KRAB} repressor screen in A431 cells was not found to modulate HER2 expression in the dCas9^{p300} gain-of-function screen in HEK293T cells, which we further validated with individual gRNAs (**Supplementary Fig. 7c**,**d**). However, when we carried out the same gain-of-function screen in A431 cells (**Supplementary Figs. 8** and **9**), this intronic DHS was selected, which indicates that although many of the regulatory elements we found were shared between cell types, some may be cell-type specific (**Fig. 5**). This finding indicates that certain cell types have complex and possibly redundant patterns of regulatory element usage, and that CERES can be used to determine cell-type-specific enhancer activity. Additionally, the DHSs near the *GRB7* promoter that were identified in the dCas9^{KRAB} screen were not enriched in the A431 dCas9^{p300} screen (**Fig. 6**). This indicates that active regulatory elements might not be identified in gain-of-function screens, and repressed elements might not be identified in

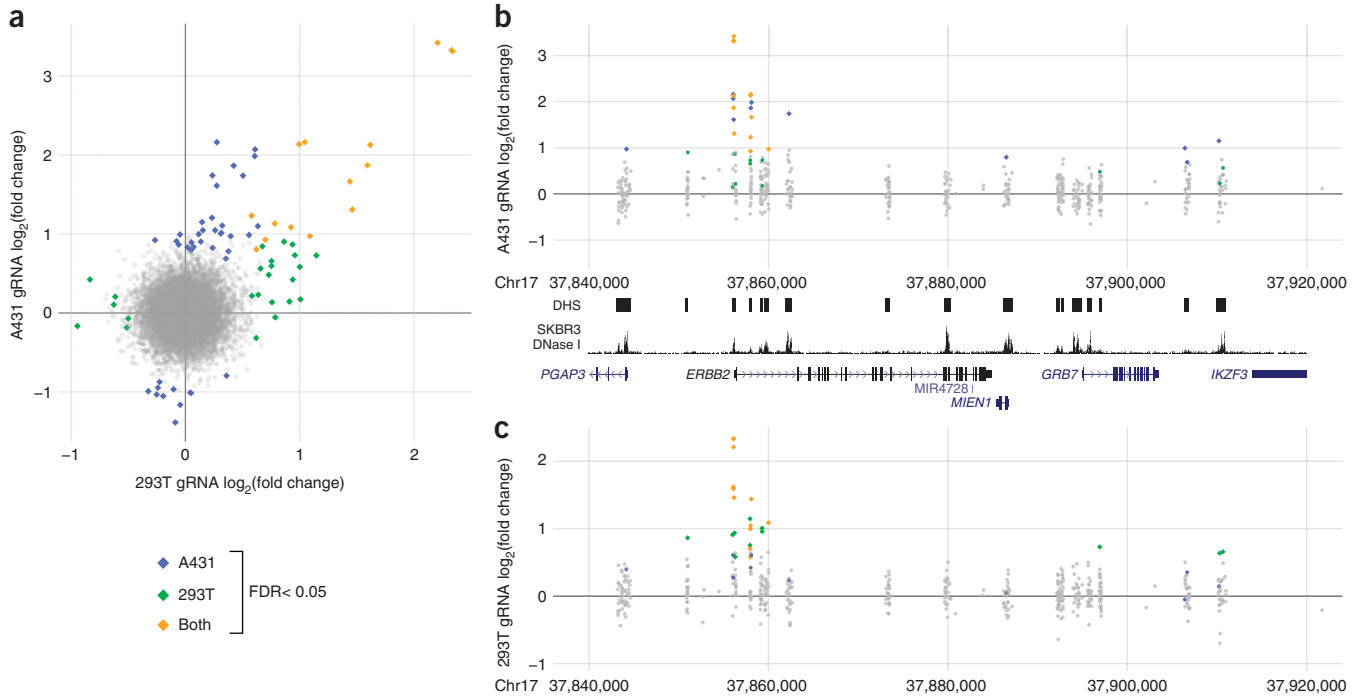

Figure 5 Comparison of HER2-activation screens in different cell types. (**a**) Log_2 fold-change gRNA abundance in the dCas9^{p300} screen in HEK293T cells versus A431 cells. (**b**,**c**) Detailed views of the region around *HER2* for the dCas9^{p300} screens in (**b**) A431 cells and (**c**) HEK293T cells. Several of the same DHSs contained enriched gRNAs in both screens, including the promoter region, but others, such as an intronic DHS highly enriched in the dCas9^{KRAB} screen in A431 cells, were enriched in only a single screen and may be cell-type-specific enhancers. Gray circles in **b**,**c** represent gRNAs that were not significantly enriched. $n = 3$ (A431-dCas9^{p300} screen) or 4 (293T-dCas9^{p300} screen) biological replicates.

loss-of-function screens. This also underscores the need for the combination of repression and activation screens to provide a comprehensive description of gene regulation. Future iterations of the CERES technology, including combinatorial screens that combine activation and repression or that target multiple regulatory elements simultaneously, may help to elucidate these patterns.

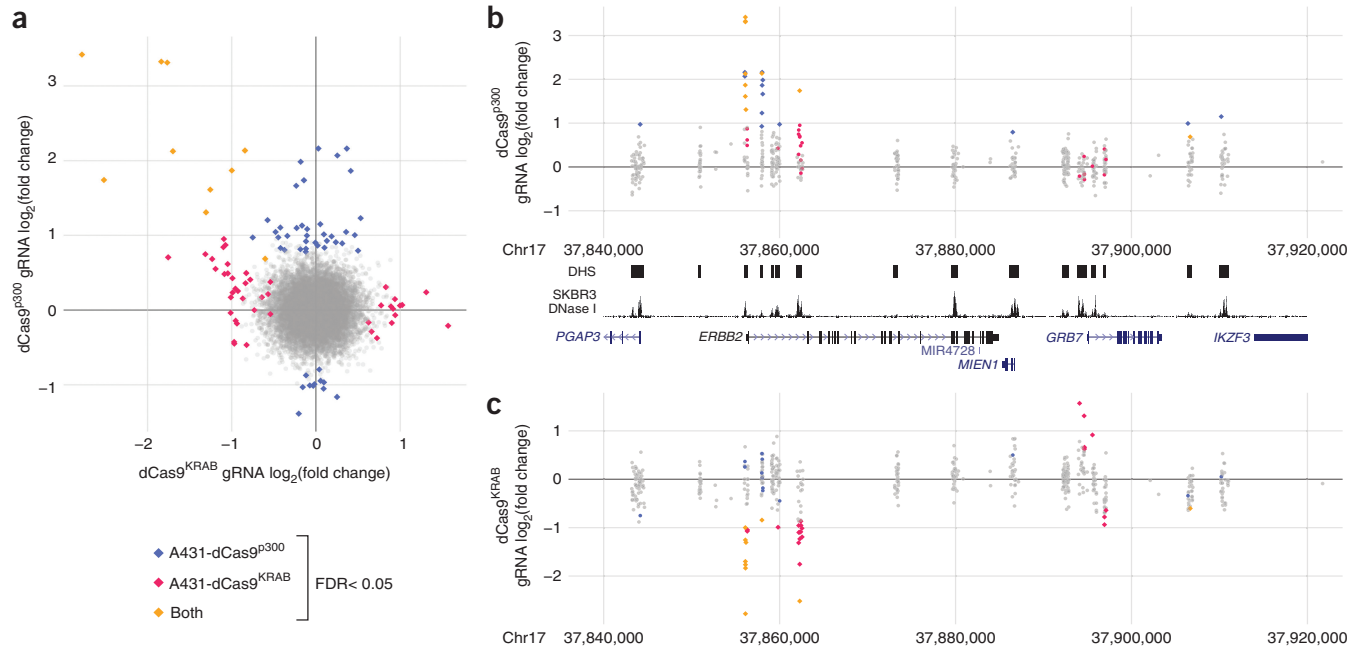

Figure 6 Comparison of HER2 activation and repression screens. (**a**) Log_2 fold change of the gRNA abundance in the dCas9^{KRAB} screen versus the dCas9^{p300} screen in A431 cells. (**b**,**c**) A detailed view of the region around *HER2* for the (**b**) dCas9^{p300} and (**c**) dCas9^{KRAB} screens in A431 cells. Several DHSs contained enriched gRNAs in both screens, including the promoter and *HER2*-intronic DHSs. However, DHSs in the *GRB7* promoter region were enriched only in the dCas9^{KRAB} screen. Gray circles in **b**,**c** represent gRNAs that were not significantly enriched. $n = 3$ (A431-dCas9^{p300} screen) or 4 (A431-dCas9^{KRAB} screen) biological replicates.

DISCUSSION

New technologies are necessary to address the unique challenges of annotating the function of regulatory elements, in contrast to the well-established methods for screening protein-coding genes. Current models of gene regulation often involve multiple regulatory elements that individually may have modest effects on promoter activity but collectively synergize to generate robust gene expression programs in response to complex cellular environments and signals. In those models, the perturbations of individual elements in screens such as CERES are likely to have subtle effects, particularly compared with gene-knockout screens or screens that target gene promoters. Indeed, few of the gRNAs in our screens drove a change of more than twofold in gene expression (**Figs. 2c** and **3c**). Nevertheless, targeted validation experiments confirmed that these gRNAs are in fact modulators of target gene expression (**Supplementary Figs. 5**, **7**, and **9**). Furthermore, many of the other gRNAs in those DHSs had a consistent direction of effect (e.g., DHS 1561 (**Fig. 2c**) and DHS 1563 (**Fig. 3c**); also see **Supplementary Fig. 10**). This finding is consistent with individual regulatory elements having a weak effect on target gene expression, and shows that the CERES protocol can reproducibly detect such weak effects. Nonetheless, it is possible that our current protocol may miss some of the weak effects of regulatory elements. That limitation could be addressed in the future by improvements to epigenome editing tools and by increasing the sample size beyond the four biological replicates used here.

Fulco *et al.*[49] recently reported a similar loss-of-function screen for regulatory elements, using the dCas9^{KRAB} repressor. In their study they used all gRNAs tiled along a particular genomic region, whereas we focused on putative regulatory elements, such as those defined by DNase-seq. Targeting DHSs allowed us to focus on a much larger genomic window per gRNA, which may be useful for identifying long-range interactions or indirect effects of regulatory elements on a particular gene or phenotype. Although Fulco *et al.*[49] observed strong correlation of functional regulatory elements with DNase-seq signal, other studies using Cas9-based saturation mutagenesis of noncoding regions found some hits that were not characterized by DNase I hypersensitivity[18,20]. In the context of the gain-of-function dCas9^{p300} screen, we compared our DHS-focused approach to a saturation screen that included all possible unique gRNAs in a 60-kb window around the HER2 transcription start site and all possible gRNAs in all DHSs that included any hits in the original screen (**Supplementary Figs. 11** and **12**). The results largely overlapped, albeit with some differences, which indicates that it is valuable to choose the gRNA distribution that best suits a particular screen.

To better understand the differences of Cas9-based mutagenesis screens and epigenome-editing-based screens, we used this same saturation library with an analogous Cas9 vector and compared the results with those from the original DHS-focused dCas9^{KRAB} screen (**Supplementary Figs. 13–15**). The hits in the Cas9 screen were predominantly in the coding exons (**Supplementary Fig. 13**), and even the known regulatory elements were missed in that screen (**Supplementary Fig. 14**), which supports the advantages of an epigenome editing approach.

In summary, we show that CERES offers a highly scalable epigenome-editing-based platform that enables parallel loss- and gain-of-function methods to screen for the function of regulatory regions of the genome in their native genomic context. CERES can identify both proximal and distal regulatory elements that influence gene expression, some of which are located large distances from their target genes. Using CERES, we found all the known regulatory elements of the well-characterized β-globin locus, and also known and—to our knowledge—previously unknown elements that control expression levels of the oncogene *HER2*. In addition to identifying enhancers, CERES also identifies regulatory elements that may act through direct competition with the promoter region or through downstream secondary mechanisms. The ability to switch between screens that utilize either epigenomic repression by dCas9^{KRAB} or activation by dCas9^{p300} allows further mechanistic understanding of regulatory element activity, and reveals unexpected dependencies between genes. In addition, these results provide evidence that dCas9^{p300} is sufficient to activate gene expression from distal regulatory elements. After large-scale screens to identify regulatory element function with CERES, saturation mutagenesis screens with genome editing could be carried out on targeted regulatory elements to identify the essential transcription-factor-binding motifs that facilitate enhancer activity[16–20,50]. Although this study used chromatin-accessibility DNase-seq maps to define the regulatory element landscape, the gRNA library could be designed on the basis of any input, including locations from chromatin immunoprecipitation followed by sequencing (ChIP-seq), global run-on sequencing (GRO-seq), or single-nucleotide polymorphisms identified in genome-wide association studies or analyses of expression quantitative trait loci. The gRNA library may target all putative regulatory elements, or elements with differential epigenetic signatures between cell types or treatments.

Additionally, CERES could be used to screen for regulatory elements that affect cellular phenotype, including drug resistance or cell growth. Although we targeted gRNA libraries to putative regulatory elements within a region of the genome, scaling up to regulatory elements across the entire genome is feasible. Our study shows that epigenome-editing-based screening is a powerful tool for dissecting the regulatory networks that coordinate gene expression. Ultimately, we envision that these methods will provide information on how altered regulation of gene expression contributes to disease, drug response, and regeneration. We also expect that by illuminating the function of the noncoding genome, these technologies will provide a new class of drug targets for diverse indications.

METHODS

Methods, including statements of data availability and any associated accession codes and references, are available in the online version of the paper.

Note: Any Supplementary Information and Source Data files are available in the online version of the paper.

ACKNOWLEDGMENTS

This work was supported by the Thorek Memorial Foundation, the US National Institutes of Health (NIH) (grants R01DA036865, R41GM119914, and U01HG007900 to G.E.C., T.E.R., and C.A.G.; core facility grant P30AR066527; Biotechnology Training Grant T32GM008555 to T.S.K. and J.B.B.; Director's New Innovator Award DP2OD008586 to C.A.G.), and the National Science Foundation (NSF) (Faculty Early Career Development (CAREER) Award CBET-1151035 to C.A.G.).

AUTHOR CONTRIBUTIONS

T.S.K., G.E.C., T.E.R., and C.A.G. designed experiments. T.S.K., J.B.B., A.S., L.S., and M.C. performed the experiments. I.B.H. provided critical reagents. T.S.K., G.E.C., T.E.R., and C.A.G. analyzed the data. T.S.K. and C.A.G. wrote the manuscript, with contributions by all others authors.

COMPETING FINANCIAL INTERESTS

The authors declare competing financial interests: details are available in the online version of the paper.

1. Thurman, R.E. *et al.* The accessible chromatin landscape of the human genome. *Nature* **489**, 75–82 (2012).
2. Hindorff, L.A., Junkins, H.A., Mehta, J.P. & Manolio, T.A. A Catalog of Published Genome-Wide Association Studies. http://www.genome.gov/gwastudies (2009).
3. ENCODE Project Consortium. An integrated encyclopedia of DNA elements in the human genome. *Nature* **489**, 57–74 (2012).
4. Bernstein, B.E. *et al.* The NIH Roadmap Epigenomics Mapping Consortium. *Nat. Biotechnol.* **28**, 1045–1048 (2010).
5. Arnold, C.D. *et al.* Genome-wide quantitative enhancer activity maps identified by STARR-seq. *Science* **339**, 1074–1077 (2013).
6. Vockley, C.M. *et al.* Massively parallel quantification of the regulatory effects of noncoding genetic variation in a human cohort. *Genome Res.* **25**, 1206–1214 (2015).
7. Vockley, C.M. *et al.* Direct GR binding sites potentiate clusters of TF binding across the human genome. *Cell* **166**, 1269–1281 (2016).
8. Barrangou, R. & Doudna, J.A. Applications of CRISPR technologies in research and beyond. *Nat. Biotechnol.* **34**, 933–941 (2016).
9. Jinek, M. *et al.* A programmable dual-RNA-guided DNA endonuclease in adaptive bacterial immunity. *Science* **337**, 816–821 (2012).
10. Cong, L. *et al.* Multiplex genome engineering using CRISPR/Cas systems. *Science* **339**, 819–823 (2013).
11. Mali, P. *et al.* RNA-guided human genome engineering via Cas9. *Science* **339**, 823–826 (2013).
12. Cho, S.W., Kim, S., Kim, J.M. & Kim, J.-S. Targeted genome engineering in human cells with the Cas9 RNA-guided endonuclease. *Nat. Biotechnol.* **31**, 230–232 (2013).
13. Shalem, O. *et al.* Genome-scale CRISPR-Cas9 knockout screening in human cells. *Science* **343**, 84–87 (2014).
14. Wang, T., Wei, J.J., Sabatini, D.M. & Lander, E.S. Genetic screens in human cells using the CRISPR-Cas9 system. *Science* **343**, 80–84 (2014).
15. Koike-Yusa, H., Li, Y., Tan, E.P., Del Castillo Velasco-Herrera, M. & Yusa, K. Genome-wide recessive genetic screening in mammalian cells with a lentiviral CRISPR-guide RNA library. *Nat. Biotechnol.* **32**, 267–273 (2014).
16. Canver, M.C. *et al.* BCL11A enhancer dissection by Cas9-mediated *in situ* saturating mutagenesis. *Nature* **527**, 192–197 (2015).
17. Korkmaz, G. *et al.* Functional genetic screens for enhancer elements in the human genome using CRISPR-Cas9. *Nat. Biotechnol.* **34**, 192–198 (2016).
18. Rajagopal, N. *et al.* High-throughput mapping of regulatory DNA. *Nat. Biotechnol.* **34**, 167–174 (2016).
19. Diao, Y. *et al.* A new class of temporarily phenotypic enhancers identified by CRISPR/Cas9-mediated genetic screening. *Genome Res.* **26**, 397–405 (2016).
20. Sanjana, N.E. *et al.* High-resolution interrogation of functional elements in the noncoding genome. *Science* **353**, 1545–1549 (2016).
21. Vierstra, J. *et al.* Functional footprinting of regulatory DNA. *Nat. Methods* **12**, 927–930 (2015).
22. Housden, B.E. *et al.* Loss-of-function genetic tools for animal models: cross-species and cross-platform differences. *Nat. Rev. Genet.* **18**, 24–40 (2017).
23. Thakore, P.I., Black, J.B., Hilton, I.B. & Gersbach, C.A. Editing the epigenome: technologies for programmable transcription and epigenetic modulation. *Nat. Methods* **13**, 127–137 (2016).
24. Qi, L.S. *et al.* Repurposing CRISPR as an RNA-guided platform for sequence-specific control of gene expression. *Cell* **152**, 1173–1183 (2013).
25. Gilbert, L.A. *et al.* CRISPR-mediated modular RNA-guided regulation of transcription in eukaryotes. *Cell* **154**, 442–451 (2013).
26. Gao, X. *et al.* Reprogramming to pluripotency using designer TALE transcription factors targeting enhancers. *Stem Cell Reports* **1**, 183–197 (2013).
27. Gao, X. *et al.* Comparison of TALE designer transcription factors and the CRISPR/dCas9 in regulation of gene expression by targeting enhancers. *Nucleic Acids Res.* **42**, e155 (2014).
28. Gilbert, L.A. *et al.* Genome-scale CRISPR-mediated control of gene repression and activation. *Cell* **159**, 647–661 (2014).
29. Konermann, S. *et al.* Genome-scale transcriptional activation by an engineered CRISPR-Cas9 complex. *Nature* **517**, 583–588 (2015).
30. Hilton, I.B. *et al.* Epigenome editing by a CRISPR-Cas9-based acetyltransferase activates genes from promoters and enhancers. *Nat. Biotechnol.* **33**, 510–517 (2015).
31. Kearns, N.A. *et al.* Functional annotation of native enhancers with a Cas9-histone demethylase fusion. *Nat. Methods* **12**, 401–403 (2015).
32. Thakore, P.I. *et al.* Highly specific epigenome editing by CRISPR-Cas9 repressors for silencing of distal regulatory elements. *Nat. Methods* **12**, 1143–1149 (2015).
33. Xu, X. *et al.* A CRISPR-based approach for targeted DNA demethylation. *Cell Discov.* **2**, 16009 (2016).
34. Choudhury, S.R., Cui, Y., Lubecka, K., Stefanska, B. & Irudayaraj, J. CRISPR-dCas9 mediated TET1 targeting for selective DNA demethylation at *BRCA1* promoter. *Oncotarget* **7**, 46545–46556 (2016).
35. Vojta, A. *et al.* Repurposing the CRISPR-Cas9 system for targeted DNA methylation. *Nucleic Acids Res.* **44**, 5615–5628 (2016).
36. Mali, P. *et al.* CAS9 transcriptional activators for target specificity screening and paired nickases for cooperative genome engineering. *Nat. Biotechnol.* **31**, 833–838 (2013).
37. Liu, X.S. *et al.* Editing DNA methylation in the mammalian genome. *Cell* **167**, 233–247 (2016).
38. Boyle, A.P. *et al.* High-resolution mapping and characterization of open chromatin across the genome. *Cell* **132**, 311–322 (2008).
39. Sabo, P.J. *et al.* Genome-scale mapping of DNase I sensitivity *in vivo* using tiling DNA microarrays. *Nat. Methods* **3**, 511–518 (2006).
40. Hardison, R. *et al.* Locus control regions of mammalian β-globin gene clusters: combining phylogenetic analyses and experimental results to gain functional insights. *Gene* **205**, 73–94 (1997).
41. Baron, M.H. Developmental regulation of the vertebrate globin multigene family. *Gene Expr.* **6**, 129–137 (1996).
42. Dean, A., Ley, T.J., Humphries, R.K., Fordis, M. & Schechter, A.N. Inducible transcription of five globin genes in K562 human leukemia cells. *Proc. Natl. Acad. Sci. USA* **80**, 5515–5519 (1983).
43. Song, L. *et al.* Open chromatin defined by DNaseI and FAIRE identifies regulatory elements that shape cell-type identity. *Genome Res.* **21**, 1757–1767 (2011).
44. Vu, T. & Claret, F.X. Trastuzumab: updated mechanisms of action and resistance in breast cancer. *Front. Oncol.* **2**, 62 (2012).
45. Slamon, D.J. *et al.* Use of chemotherapy plus a monoclonal antibody against HER2 for metastatic breast cancer that overexpresses HER2. *N. Engl. J. Med.* **344**, 783–792 (2001).
46. Gajria, D. & Chandarlapaty, S. HER2-amplified breast cancer: mechanisms of trastuzumab resistance and novel targeted therapies. *Expert Rev. Anticancer Ther.* **11**, 263–275 (2011).
47. Hurtado, A. *et al.* Regulation of ERBB2 by oestrogen receptor-PAX2 determines response to tamoxifen. *Nature* **456**, 663–666 (2008).
48. Chu, P.-Y., Li, T.-K., Ding, S.-T., Lai, I.R. & Shen, T.-L. EGF-induced Grb7 recruits and promotes Ras activity essential for the tumorigenicity of Sk-Br3 breast cancer cells. *J. Biol. Chem.* **285**, 29279–29285 (2010).
49. Fulco, C.P. *et al.* Systematic mapping of functional enhancer-promoter connections with CRISPR interference. *Science* **354**, 769–773 (2016).
50. Findlay, G.M., Boyle, E.A., Hause, R.J., Klein, J.C. & Shendure, J. Saturation editing of genomic regions by multiplex homology-directed repair. *Nature* **513**, 120–123 (2014).

ONLINE METHODS

Plasmids. We generated the lentiviral dCas9^{KRAB} (Addgene, 83890) plasmid by cloning in a hygromycin-resistance gene driven by the PGK promoter after dCas9^{KRAB} using Gibson assembly (NEB, E2611L). We cloned the lentiviral gRNA expression plasmid by combining a U6-gRNA cassette with an EGFP-P2A-Bsr (Addgene, 83925) or DsRed-P2A-Bsr (Addgene, 83919) cassette into a lentiviral expression backbone by Gibson assembly. We cloned the donor plasmid by inserting homology arms (surrounding the *HBE1* stop codon), amplified by PCR from genomic DNA of K562 cells, flanking a P2A–mCherry sequence with a LoxP-puromycin resistance cassette by Gibson assembly. Individual gRNAs were ordered as oligonucleotides (IDT-DNA), phosphorylated, hybridized, and cloned into the EGFP gRNA plasmid for the HBE1 screen or into the DsRed gRNA plasmid for the HER2 screens using BsmBI sites.

The lentiviral dCas9^{p300} (Addgene, 83889) construct was generated by PCR amplification of Cas9 from lentiCRISPRv2 (ref. 51) (Addgene, 52961) with primers that generated D10A and H840A mutations in overlapping fragments. The p300 core effector domain was PCR-amplified from Addgene, 61357 (ref. 30), with a C-terminal Flag epitope included. These fragments were cloned into a lentiCRISPRv2 backbone lacking the U6/sgRNA cassette by Gibson assembly (NEB, E2611L).

Cell culture. K562, HEK293T, and A431 cells were obtained from the American Type Culture Collection (ATCC) via the Duke University Cancer Center facilities. K562 cells were maintained in RPMI 1640 media supplemented with 10% FBS and 1% penicillin–streptomycin. HEK293T and A431 cells were maintained in DMEM High Glucose supplemented with 10% FBS and 1% penicillin–streptomycin. All cell lines were cultured at 37 °C and 5% CO_2.

The K562-dCas9^{KRAB} HBE1 reporter cell line was generated by electroporation of 2×10^6 cells with a donor plasmid (6.67 µg), an *HBE1* stop-codon-targeting gRNA plasmid (6.67 µg), and a Cas9 plasmid (6.67 µg), as described previously[32]. Transfected cells were selected with puromycin (Sigma, P8833) at a concentration of 1 µg/mL, beginning 2 d after electroporation, for 7 d. To remove the puromycin selection cassette, we transfected cells with a CMV-Cre plasmid (20 µg) and cultured them for 10 d without antibiotic selection. Next, we transduced the cells with a lentivirus containing dCas9^{KRAB} in media that contained 4 µg/mL polybrene (Santa Cruz Biotechnology, sc-134220). Cells were selected with hygromycin B (200 µg/mL) for 7 d. Cells were then clonally isolated via serial dilution to obtain a single clone that harbored the knocked-in reporter without the puromycin cassette and dCas9^{KRAB}.

We derived the A431-dCas9^{p300} and HEK293T-dCas9^{p300} cell lines by transducing either A431 or HEK293T cells with a lentivirus that contained dCas9^{p300}-P2A-puromycin and, 2 d after transduction, selecting with puromycin for 7 d.

DNase-seq. DNase-seq was carried out on the SKBR3 cell line as previously described[52], with the addition of phosphorylation modification to linker 1b to increase the ligation efficiency.

gRNA library design and cloning. DHSs for the K562 cell line were downloaded from ENCODE (http://www.encodeproject.org), and SKBR3 DHS regions were obtained as described earlier and used to extract genomic sequences as input for gRNA identification. For each cell line's set of DHSs, we used the gt-scan algorithm to identify gRNA protospacers within each DHS region and identify possible alignments to other regions of the genome[53]. The result was a database that contained all possible gRNAs targeting all DHSs in the given cell line, and each gRNA's possible off-target locations. For both libraries, gRNAs were selected with the goal of minimizing off-target alignments. For the HBE1 library, we selected 10,739 gRNAs, targeting 281 DHSs surrounding *HBE1*, limited to a maximum of 50 gRNAs per DHS. For the HER2 library, we selected 12,189 gRNAs, targeting 433 DHSs surrounding *HER2*, limited to a maximum of 30 gRNAs per DHS. For each library, we designed controls by searching for gRNAs in non-DHS regions. For the HBE1 library, 1,733 gRNAs were selected, and for the HER2 library, 283 gRNAs were selected. For the saturation library targeting a 60-kb region surrounding the *HER2* promoter and DHSs containing at least one significantly enriched gRNA identified in the dCas9^{KRAB} and dCas9^{p300} screens, all gRNAs within those regions were selected except those that had perfect alignment to another area of the genome. All libraries were synthesized by Custom Array, and the oligo pools were cloned into the lentiviral gRNA expression plasmid by Gibson assembly as described by Shalem *et al.*[13], with minor modifications.

Lentivirus production and titration. For the gRNA libraries and dCas9^{KRAB}, we produced lentivirus by transfecting 5×10^6 HEK293T cells with the lentiviral gRNA expression plasmid pool or dCas9^{KRAB} plasmid (20 µg), psPAX2 (Addgene, 12260; 15 µg), and pMD2.G (Addgene, 12259; 6 µg) using calcium phosphate precipitation[54]. After 14–20 h, we replaced the transfection media with fresh media. Media containing produced lentivirus was collected 24 and 48 h later. The lentivirus was concentrated at 20× the initial media volume with Lenti-X concentrator (Clontech, 631232) according to the manufacturer's instructions.

We determined the titer of the lentivirus containing either the HBE1 or HER2 pool of gRNAs by transducing 4×10^5 cells with varying volumes of lentivirus and measuring the level of GFP or DsRed 4 d later with a MACSQuant VYB flow cytometer (Miltenyi Biotec) to determine the percent transduction.

For dCas9^{p300}, we transfected 15×10^6 HEK293T cells with dCas9^{p300} plasmid (120 µg), psPAX2 (90 µg), and pMD2.G (36 µg) using calcium phosphate precipitation. After 14–20 h, the transfection media was replaced with fresh media, and 24 h after that, the media was harvested. The lentivirus was pooled by ultracentrifugation (Beckman) at 24,000 r.p.m. for 2 h at 4 °C. The lentiviral pellet was resuspended in 1× PBS overnight to achieve a concentration of 400×.

To produce lentivirus for individual gRNA validations, we transfected 2×10^5 cells with gRNA plasmid (200 ng), psPAX2 (600 ng), and pMD2.G (200 ng) using Lipofectamine 2000 according to the manufacturer's instructions. After 14–20 h, the transfection media was replaced with fresh media. Media containing produced lentivirus was harvested 24 and 48 h later, centrifuged for 10 min at 800*g*, and used directly to transduce cells.

Lentiviral gRNA screening. For all screens, 6.236×10^6 cells were transduced during seeding in a 15-cm dish in 20 mL of media supplemented with 4 µg/mL polybrene across four replicates, except the A431-dCas9^{p300} HER2 screen targeting DHSs, which was performed across three replicates. We transduced cells at an MOI of 0.2 to try to achieve 1 gRNA per cell and 100-fold coverage of each gRNA library. After 2 d, cells were treated with blasticidin S (Thermo Fisher, A1113903) at a concentration of 20 µg/mL. Cells were grown for an additional 12 d for the dCas9^{KRAB} screen targeting DHSs of the *HBE1* locus, an additional 9 (**Supplementary Fig. 16**) or 17 d for the dCas9^{KRAB} screen targeting DHSs of the *HER2* locus in A431 cells, and an additional 7 d for the dCas9^{p300} screen targeting DHSs or saturating a 60-kb region of the *HER2* locus in HEK293T or A431 cells. For the Cas9 screen targeting a 60-kb region surrounding the *HER2* promoter and all DHSs containing enriched gRNAs in the dCas9^{KRAB} screen with all possible gRNAs in A431 cells, cells were grown an additional 9 d. Cells were passaged to ensure adequate fold coverage of the gRNA library to maintain representation. After culturing, 5×10^7 K562 cells were harvested, washed once with PBS, and resuspended in DMEM without phenol red and supplemented with 100 units of DNase I (NEB, M0303S) for sorting. For HEK293T or A431 cells, 5×10^7 cells were harvested with 0.25% Trypsin-EDTA (Thermo Fisher, 25200056) and resuspended in 5% goat serum in PBS to block for 30 min at 4 °C. Next, cells were incubated in 125 µg of HER2 primary antibody (monoclonal mouse IgG2B, clone 191924, R&D Systems) in 5 mL of 5% goat serum in PBS for 30 min at 4 °C. Cells were then washed once in PBS and resuspended in secondary antibody (goat anti-mouse IgG2b, Alexa Fluor 488 conjugate, Thermo Fisher, A-21141) diluted 1:500 in 5 mL of 5% goat serum in PBS and incubated for 30 min at 4 °C. Finally, cells were washed once with PBS and resuspended in DMEM without phenol red supplemented with 100 units of DNase I for sorting.

We took an aliquot of 1.3×10^6 cells before sorting for a bulk unsorted sample for each screen. The highest and lowest 10% of cells were sorted on the basis of mCherry signal for the dCas9^{KRAB} screen of *HBE1* in K562 cells, or Alexa Fluor 488 signal for all HER2 screens. 1.3×10^6 cells were sorted for each group. Cell sorting was done with a MoFlo Astrios (Beckman Coulter) or SH800 (Sony Biotechnology). After sorting, cells were harvested for genomic DNA with the DNeasy Blood and Tissue Kit (Qiagen, 69506).

Genomic DNA sequencing. To amplify the gRNA libraries from each sample, we used 8.3 µg of gDNA as a template across eight 100-µL PCR reactions using Q5 hot start polymerase (NEB, M0493L). We carried out amplification according to the manufacturer's instructions, using 25 cycles at an annealing temperature of 60 °C with the following primers:

Fwd: 5′-AATGATACGGCGACCACCGAGATCTACACAATTTCTTGGGTAGTTTGCAGTT

Rev: 5′-CAAGCAGAAGACGGCATACGAGAT-(6-bp index sequence)-GACTCGGTGCCACTTTTTCAA

We purified the amplified libraries with Agencourt AMPure XP beads (Beckman Coulter, A63881) using double size selection of 0.65× and then 1× the original volume. Each sample was quantified after purification with the Qubit dsDNA High Sensitivity assay kit (Thermo Fisher, Q32854). Samples were pooled and sequenced on a MiSeq (Illumina) with 21-bp paired-end sequencing using the following custom read and index primers:

Read1: 5′-GATTTCTTGGCTTTATATATCTTGTGGAAAGGACGAAACACCG

Index: 5′-GCTAGTCCGTTATCAACTTGAAAAAGTGGCACCGAGTC

Read2: 5′-GTTGATAACGGACTAGCCTTATTTTAACTTGCTATTTCTAGCTCTAAAAC

Data processing and enrichment analysis. We aligned FASTQ files to custom indexes (generated from the bowtie2-build function) using Bowtie 2 (ref. 55) with the options -p 32 --end-to-end --very-sensitive -3 1 -I 0 -X 200. Counts for each gRNA were extracted and used for further analysis. All enrichment analysis was done with R. For DHS-level analysis, we grouped gRNAs for each DHS together and used a linear regression model (normalized_gRNA_count = β_1*(sorted_bin) + β_2*(replicate)) to detect differences between the high and low conditions using the Holm method for multiple hypothesis correction. For individual gRNA enrichment analysis, we used the DESeq2 (ref. 56) package to compare between high and low, unsorted and low, or unsorted and high conditions for each screen.

Individual gRNA validations. The protospacers from the top enriched gRNAs found in each screen (**Supplementary Tables 3** and **4**) were ordered as oligonucleotides from IDT and cloned into a lentiviral gRNA expression vector as described earlier. The same modified cell lines used in the corresponding screen were used for the individual gRNA validations. The cells were transduced with individual gRNAs, and after 2 d they were selected with blasticidin S (20 µg/mL). We transduced samples with combinations of gRNAs by delivering an equal volume of viral supernatant of each gRNA. Cells were selected for 12 d for the HBE1 dCas9^{KRAB} screen hits, 9 d for the HER2 dCas9^{KRAB} screen hits, and 7 d for the HER2 dCas9^{p300} screen hits.

For all screen validations, mRNA expression was done in triplicate. Total mRNA was harvested from cells with the Qiagen RNeasy Plus mini kit (Qiagen, 74136). cDNA was generated with the SuperScript VILO cDNA synthesis kit (Thermo Fisher, 11754250). qRT-PCR was done with Perfecta SYBR Green FastMix (Quanta Biosciences, 95072-012) with the FX96 real-time PCR detection system (Bio-Rad), with the primers listed in **Supplementary Table 5**. The results are expressed as fold-increase mRNA expression of the gene of interest normalized to *GAPDH* expression by the $\Delta\Delta C_t$ method.

For flow cytometry analysis of the HBE1 dCas9^{KRAB} screen validations, cells were harvested, washed once in PBS, and resuspended in PBS. For the HER2 dCas9^{KRAB} and dCas9^{p300} screen validations, cells were harvested, washed once with PBS, resuspended in 5% goat serum in PBS and blocked for 30 min at 4 °C. HER2 primary antibody (monoclonal mouse IgG2B, clone 191924, R&D Systems) was then added and allowed to incubate for 30 min at 4 °C. Cells were then washed once in 5% goat serum in PBS. Secondary antibody (goat anti-mouse IgG2b, Alexa Fluor 488 conjugate, Thermo Fisher, A-21141) was then added, and cells were allowed to incubate at 4 °C for 30 min. Cells were then washed once in PBS. All cells were analyzed with a MACSQuant VYB flow cytometer (Miltenyi Biotec).

ChIP-qPCR. The same cell lines used in the screens described earlier were used for ChIP-qPCR experiments: H3K27ac samples used HEK293T cells expressing dCas9^{p300}, and H3K9me3 samples used A431 cells expressing dCas9^{KRAB}. Cells were transduced with lentivirus containing gRNAs (**Supplementary Table 6**) and allowed to grow for 9 d for H3K27ac samples or 11 d for H3K9me3 samples. Cells were fixed in 1% formaldehyde for 10 min at room temperature. The reaction was quenched with 0.125 M glycine, and the cells were lysed with Farnham lysis buffer with a protease inhibitor cocktail (Roche). Nuclei were collected by centrifugation at 2,000 r.p.m. for 5 min at 4 °C and lysed in RIPA buffer with a protease inhibitor cocktail (Roche). The chromatin was sonicated with a Bioruptor sonicator (Diagenode, model XL) and immunoprecipitated with the following antibodies: anti-H3K27ac (Abcam, ab4729) and anti-H3K4me3 (Abcam, ab8580). The formaldehyde cross-links were reversed by heating overnight at 65 °C, and genomic DNA fragments were purified with a spin column. qPCR was done with SYBR Green Fastmix (Quanta BioSciences) with the CFX96 real-time PCR detection system (Bio-Rad) with primers listed in (**Supplementary Table 7**). We used 1 ng of genomic DNA in each qPCR reaction. Data are presented as the fold change in gDNA relative to the negative control and normalized to a region of the *ACTB* locus.

Data availability. DNase-seq and gRNA library sequencing data have been deposited in the NCBI Gene Expression Omnibus under accession number GSE96876.

51. Sanjana, N.E., Shalem, O. & Zhang, F. Improved vectors and genome-wide libraries for CRISPR screening. *Nat. Methods* **11**, 783–784 (2014).
52. Song, L. & Crawford, G.E. DNase-seq: a high-resolution technique for mapping active gene regulatory elements across the genome from mammalian cells. *Cold Spring Harb. Protoc.* **2010**, pdb.prot5384 (2010).
53. O'Brien, A. & Bailey, T.L. GT-Scan: identifying unique genomic targets. *Bioinformatics* **30**, 2673–2675 (2014).
54. Salmon, P. & Trono, D. Production and titration of lentiviral vectors. *Curr. Protoc. Neurosci.* Chapter 4, Unit 4.21 (2006).
55. Langmead, B. & Salzberg, S.L. Fast gapped-read alignment with Bowtie 2. *Nat. Methods* **9**, 357–359 (2012).
56. Love, M.I., Huber, W. & Anders, S. Moderated estimation of fold change and dispersion for RNA-seq data with DESeq2. *Genome Biol.* **15**, 550 (2014).

doi:10.1038/nbt.3853